



# A High Performance Multi-pulse AC-DC Converter for Adjustable Speed Motor Drives

Sharmin Shila<sup>1</sup>, Shuvra Prokash Biswas<sup>1</sup>(✉), and Md. Rabiul Islam<sup>2</sup>

<sup>1</sup> Rajshahi University of Engineering and Technology, Rajshahi 6204, Bangladesh  
spbiswas@ete.ruet.ac.bd

<sup>2</sup> University of Wollongong, Wollongong, NSW 2522, Australia  
mrislam@uow.edu.au

**Abstract.** This work includes a thorough examination in order to design a novel hexagon-connected autotransformer for a 44-pulse AC-DC converter fed vector controlled induction motor drive (VCIMD). Two paralleled twenty two-pulse AC-DC converters, each with an eleven-phase diode bridge rectifier (DBR), constitute the proposed converter. The system's performance is evaluated in MATLAB/Simulink environment under various operating conditions of the VCIMD. Traditional 6-pulse converter fed VCIMD suffers from power quality problems. This work intends to alter the design of the suggested autotransformer to make it acceptable for applications that employ a 6-pulse AC-DC converter, in order to minimize the drawbacks of 6-pulse DBR supplied VCIMD. The simulation results show that the power quality characteristics of input AC line current have been improved and are in compliance with the IEEE-519 standard. In order to justify the proposed converter's efficiency, a comparative study is also presented in comparison to existing configurations.

**Keywords:** Hexagon transformer · AC-DC converter · Power quality · 44-pulse rectifier · Vector controlled induction motor drive

## 1 Introduction

Variable frequency induction motor drives, which are utilized in a variety of applications such as compressors, pumps, air conditioning, rolling mills, and so on, have ramped up as a result of recent improvements in power-electronic converters. Vector control is the most practical means of achieving high-performance control in these induction motor drives when compared to other control techniques. This method is used in voltage source inverters, which are typically fed by six-pulse diode bridge rectifiers (DBR). The six-pulse DBR introduces harmonics in grid current, causing undesirable supply voltage circumstances and lowering power quality. The international standard IEEE-519, established in 1981, was reissued in 1992 in order to limit the harmonics fed into the grid by non-linear loads such as vector controlled induction motor drive (VCIMD) [1, 2].

Multi-pulse rectifiers have received much interest because of their ruggedness, reliability, and simplicity to implement. These methods employ two or more converters,

with harmonics produced by one converter being suppressed by the other converters due to proper phase displacement. When running at light load, the total harmonic distortion (THD) of line current for up to 18-pulse AC-DC converter topologies is more than 5%, which does not fulfill the requirements of IEEE standard. The high rating of the magnetics is also a downside of the aforementioned works. Topologies based on autotransformers, on the other hand, are capable of lowering magnetic ratings.

Various designs of autotransformer-connected multi-pulse rectifiers based on pulse doubling, phase shifting, phase multiplication, or a combination of these methods were presented in the literature [3–5]. A polygon-connected 24-pulse autotransformer with an input current THD variation of 4.15% at full load to 7.75% at light load was proposed in [3]. A hexagon-connected 20-pulse autotransformer with an input current THD variation of 4.48% at full load to 5.65% at light load was designed in [4]. In [5], another 36-pulse autotransformer with THDs of less than 5% was presented for VCIMD. However, because the voltage of the DC-link is larger than that of a 6-pulse DBR, the topology is unsuitable for retrofit applications.

For power quality enhancement, a 44-pulse AC-DC converter using a new hexagon-connected autotransformer is proposed in this work. Two 11-legged DBRs are paralleled via two interphase transformers in this configuration. As a result, the AC line current contains 44 pulses, yielding a 44-pulse output voltage. This work presents a detailed design of the entire IMD system, as well as a model and simulation of the proposed AC-DC converter in the MATLAB/Simulink environment. Different power quality characteristics are obtained and compared to a 6-pulse DBR fed system, including THD of supply voltage and current, distortion factor (DF), power factor (PF), and displacement factor (DPF).

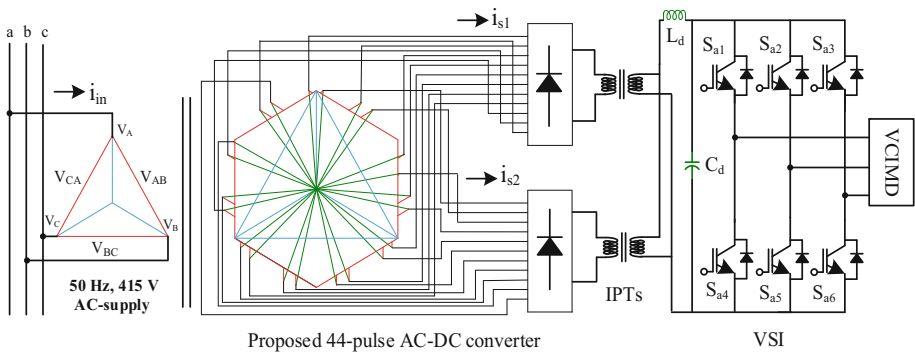


Fig. 1. Delta/Hexagon connected autotransformer configuration for 44-pulse AC-DC conversion.

## 2 Proposed 44-Pulse AC-DC Converter

The phase shift angle for a 44-pulse converter system to suppress harmonics can be evaluated as [6]:

$$\theta = \frac{360^\circ}{(N_C \times N_P)} \tag{1}$$

where  $N_C$  is the number of converters,  $N_P$  is the number of pulse, and  $\theta$  is the phase-shifted angle.

The minimum phase shift in a 44-pulse rectifier made up of two 22-pulse converters is  $8.18^\circ$ . The delta/hexagon autotransformer configured 44-pulse AC-DC converter requires a parallel connection between two 22-pulse DBRs with 11-phase shifted voltages each. The phase difference between these two sets of 11-phase voltages is  $8.18^\circ$  between the groups and  $32.725^\circ$  between the voltages of the same set. Figure 1 depicts the proposed hexagon-connected autotransformer for 44-pulse AC-DC conversion. The proposed autotransformer’s phasor diagram is shown in Fig. 2. Figure 3 illustrates the details of the hexagon transformer’s winding configuration for 44-pulse AC-DC conversion.

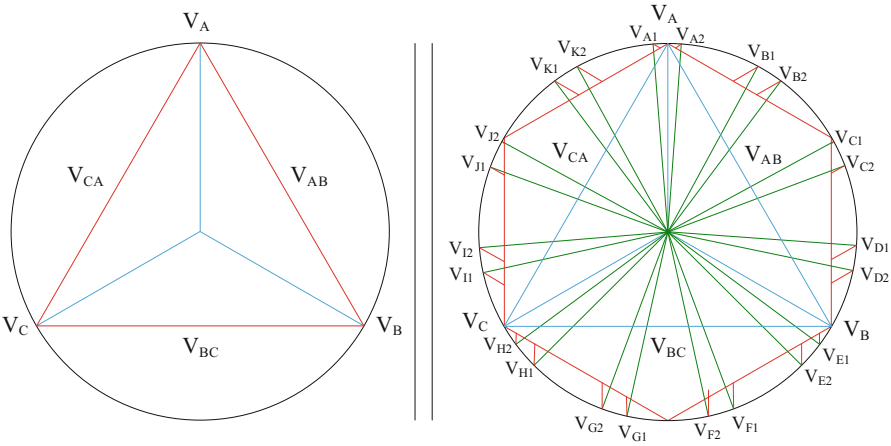


**Fig. 2.** Phasor diagram of delta/hexagon connected transformer for 44-pulse AC-DC conversion.

**2.1 Design of the Proposed Transformer**

The two voltage sets fed to DBRs are referred to as  $(V_{A1}, V_{B1}, V_{C1}, V_{D1}, V_{E1}, V_{F1}, V_{G1}, V_{H1}, V_{I1}, V_{J1}, V_{K1})$  and  $(V_{A2}, V_{B2}, V_{C2}, V_{D2}, V_{E2}, V_{F2}, V_{G2}, V_{H2}, V_{I2}, V_{J2}, V_{K2})$ . The phase shift between  $V_{A1}$  and  $V_{A2}$  is  $8.18^\circ$ . The phase displacements of  $V_{A1}$  and  $V_{A2}$  from the phase A of input voltages are  $+4.09^\circ$  and  $-4.09^\circ$ , respectively. The eleven-phase voltages are generated from AC main line and phase voltages in relation to the turns of the primary winding, as illustrated in the phasor representation in Fig. 2 and the winding arrangement in Fig. 3, which can be expressed as the following equations:

The primary winding voltages of the transformer are considered as follows:

$$V_A = V_S \angle 0^\circ, V_B = V_S \angle -120^\circ, V_C = V_S \angle +120^\circ \tag{2}$$

The eleven-phase voltages applied to the windings are:

$$V_{A1} = V_S \angle +4.09^\circ, V_{B1} = V_S \angle -28.66^\circ, V_{C1} = V_S \angle -61.385^\circ, \\ V_{D1} = V_S \angle -94.11^\circ, V_{E1} = V_S \angle -126.835^\circ, V_{F1} = V_S \angle -159.56^\circ,$$

$$\begin{aligned} V_{G1} &= V_S \angle + 167.715^\circ, V_{H1} = V_S \angle + 134.99^\circ, V_{I1} = V_S \angle + 102.265^\circ, \\ V_{J1} &= V_S \angle + 69.54^\circ, V_{K1} = V_S \angle + 36.815^\circ \end{aligned} \quad (3)$$

$$\begin{aligned} V_{A2} &= V_S \angle - 4.09^\circ, V_{B2} = V_S \angle - 36.84^\circ, V_{C2} = V_S \angle - 69.565^\circ, \\ V_{D2} &= V_S \angle - 102.29^\circ, V_{E2} = V_S \angle - 135.015^\circ, V_{F2} = V_S \angle - 167.74^\circ, \\ V_{G2} &= V_S \angle + 159.535^\circ, V_{H2} = V_S \angle + 126.81^\circ, V_{I2} = V_S \angle + 94.805^\circ, \\ V_{J2} &= V_S \angle + 61.36^\circ, V_{K2} = V_S \angle + 28.635^\circ \end{aligned} \quad (4)$$

Input voltages for 22-pulse DBR-I are:

$$\begin{aligned} V_{A1} &= V_A + K_1 V_C - K_2 V_B \\ V_{B1} &= V_A + K_3 V_B - K_4 V_C \\ V_{C1} &= V_B + K_7 V_A - K_8 V_C \\ V_{D1} &= V_B + K_{11} V_A - K_{12} V_C \\ V_{E1} &= V_B + K_{15} V_C - K_{16} V_A \\ V_{F1} &= V_B + K_{19} V_C - K_{20} V_A \\ V_{G1} &= V_C + K_{21} V_B - K_{22} V_A \\ V_{H1} &= V_C + K_{17} V_B - K_{18} V_A \\ V_{I1} &= V_C + K_{13} V_A - K_{14} V_B \\ V_{J1} &= V_C + K_9 V_A - K_{10} V_B \\ V_{K1} &= V_A + K_5 V_C - K_6 V_B \end{aligned} \quad (5)$$

Input voltages for 22-pulse DBR-II are:

$$\begin{aligned} V_{A2} &= V_A + K_1 V_B - K_2 V_C \\ V_{B2} &= V_A + K_5 V_B - K_6 V_C \\ V_{C2} &= V_B + K_9 V_A - K_{10} V_C \\ V_{D2} &= V_B + K_{13} V_A - K_{14} V_C \\ V_{E2} &= V_B + K_{17} V_C - K_{18} V_A \\ V_{F2} &= V_B + K_{21} V_C - K_{22} V_A \\ V_{G2} &= V_C + K_{19} V_B - K_{20} V_A \\ V_{H2} &= V_C + K_{15} V_B - K_{16} V_A \\ V_{I2} &= V_C + K_{11} V_A - K_{12} V_B \\ V_{J2} &= V_C + K_7 V_A - K_8 V_B \\ V_{K2} &= V_A + K_3 V_C - K_4 V_B \end{aligned} \quad (6)$$

$$V_{AB} = \sqrt{3}V_A \angle 30^\circ, V_{BC} = \sqrt{3}V_B \angle 30^\circ, V_{CA} = \sqrt{3}V_C \angle 30^\circ \quad (7)$$

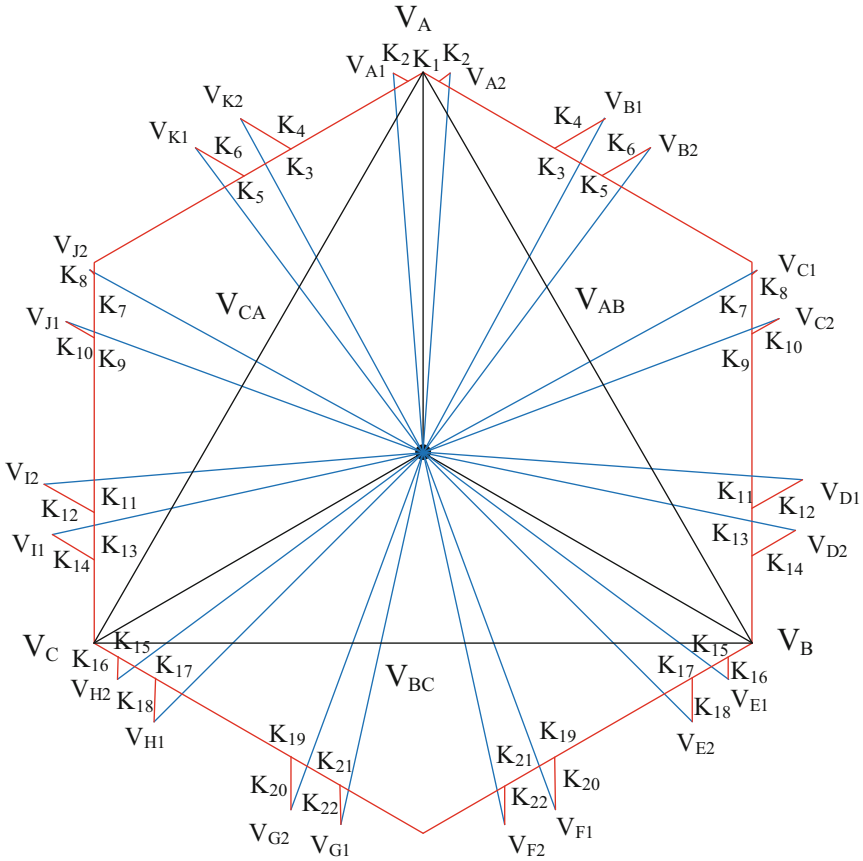


**Fig. 3.** Winding arrangement of hexagon connected transformer for 44-pulse AC-DC conversion.

**2.2 Design of the Transformer for Retrofit Applications**

The output voltage of a multi-pulse rectifier is much more DC compared to a conventional six-pulse DBR, making it unfit for retrofit applications. The output voltage of the presented 44-pulse rectifier is 20% high compared to a conventional 6-pulse DBR. Modifications to the autotransformer design result in a 20% reduction in output voltage for the proposed transformer. Modifying the tapping places as illustrated in Fig. 4, which results in the desired number of windings. The required phase shift remains the same. The following equations can be used to calculate the new tapping positions, just as they were in Sect. 2, Part 1.

Input voltages for 22-pulse DBR-I are:

$$\begin{aligned}
 V_{A1} &= V_A + K_1 V_C + K_2 V_B \\
 V_{B1} &= V_A + K_3 V_B - K_4 V_C \\
 V_{C1} &= V_B + K_7 V_A + K_8 V_C \\
 V_{D1} &= V_B + K_{11} V_A - K_{12} V_C
 \end{aligned}$$

$$\begin{aligned}
 V_{E1} &= V_B + K_{15}V_C + K_{16}V_A \\
 V_{F1} &= V_B + K_{19}V_C + K_{20}V_A \\
 V_{G1} &= V_C + K_{21}V_B + K_{22}V_A \\
 V_{H1} &= V_C + K_{17}V_B + K_{18}V_A \\
 V_{I1} &= V_C + K_{13}V_A + K_{14}V_B \\
 V_{J1} &= V_C + K_9V_A + K_{10}V_B \\
 V_{K1} &= V_A + K_5V_C + K_6V_B
 \end{aligned}
 \tag{8}$$

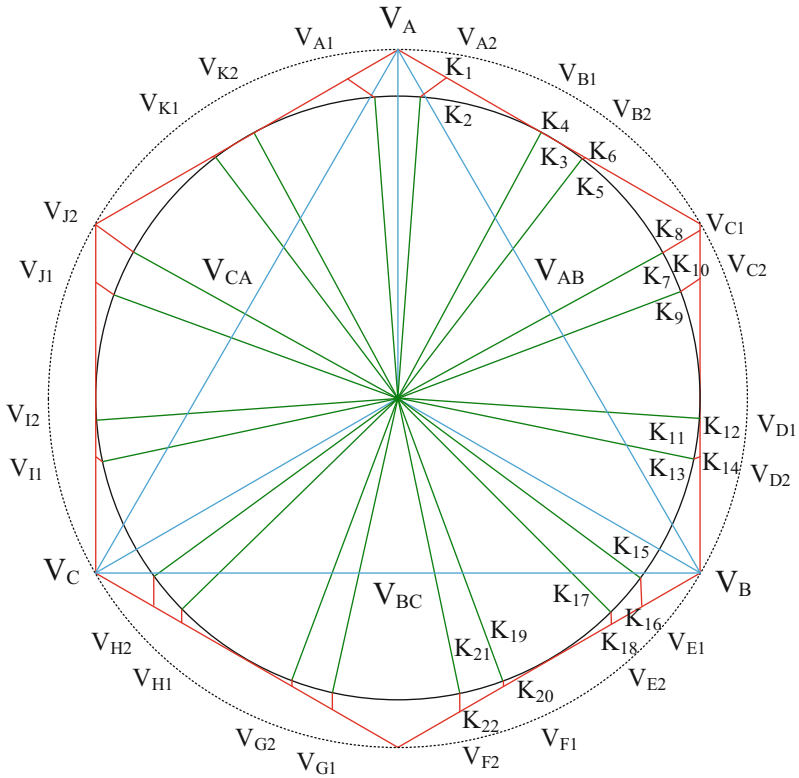


**Fig. 4.** Phasor diagram of proposed transformer for 44-pulse AC-DC conversion with modifications for retrofit applications.

Input voltages for 22-pulse DBR-II are:

$$\begin{aligned}
 V_{A2} &= V_A + K_1V_B + K_2V_C \\
 V_{B2} &= V_A + K_5V_B + K_6V_C \\
 V_{C2} &= V_B + K_9V_A + K_{10}V_C \\
 V_{D2} &= V_B + K_{13}V_A + K_{14}V_C
 \end{aligned}$$

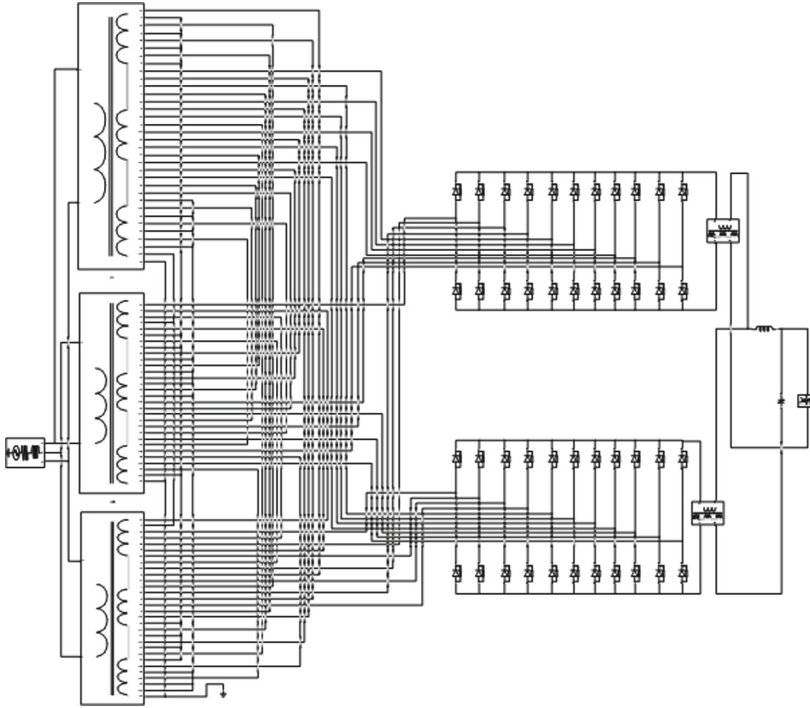


Fig. 5. MATLAB/Simulink model of the proposed 44-pulse AC-DC converter.

$$\begin{aligned}
 V_{E2} &= V_B + K_{17}V_C + K_{18}V_A \\
 V_{F2} &= V_B + K_{21}V_C + K_{22}V_A \\
 V_{G2} &= V_C + K_{19}V_B + K_{20}V_A \\
 V_{H2} &= V_C + K_{15}V_B + K_{16}V_A \\
 V_{I2} &= V_C + K_{11}V_A - K_{12}V_B \\
 V_{J2} &= V_C + K_7V_A + K_8V_B \\
 V_{K2} &= V_A + K_3V_C - K_4V_B
 \end{aligned}
 \tag{9}$$

To achieve the requisite phase shifts and output voltages, the constants  $K_1$  to  $K_{22}$  specify the secondary winding lengths as a proportion of the primary turns. As we have used the autotransformer in this work, two interphase transformers (IPTs) are connected to the DBRs to ensure that the two 22-pulse DBRs operate independently. The transformer’s kVA rating is calculated as:

$$\text{kVA} = 0.5 \sum (V_{\text{winding}} I_{\text{winding}})
 \tag{10}$$

where  $V_{\text{winding}}$  is the transformer’s winding voltage and  $I_{\text{winding}}$  is the transformer’s winding current. The apparent power rating of the IPTs is determined in the same method.

### 3 Performance Evaluation of the Presented VCIMD

The MATLAB/Simulink environment is used to design the proposed 44-pulse AC-DC converter as depicted in Fig. 5. The 44-pulse converter is supplied from a three-phase 415 V, 50 Hz AC supply. Three multi-winding transformers are utilized to model the designed transformer. The IPT is also modeled using a multi-winding transformer block. A two-level IGBT-based voltage source inverter (VSI) is connected to the converter output via the DC link consisting of a series inductor ( $L_d$ ) and capacitor ( $C_d$ ). Using a sinusoidal pulse width modulation strategy, the firing pulses for the VSI are generated. VSI drives a three-phase squirrel cage winding based induction motor using an indirect vector control technique. The output voltage of the proposed transformer's simulation model is shown in Fig. 6.

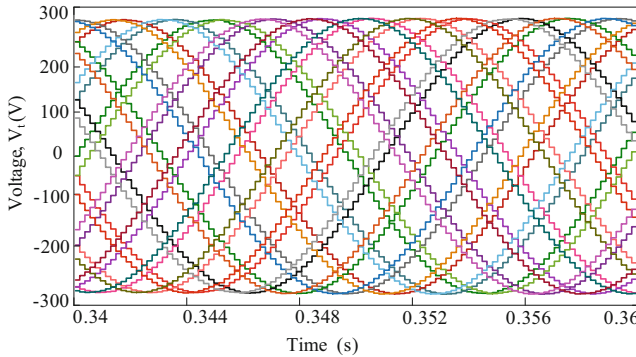


**Fig. 6.** Output voltage of the proposed transformer.

The dynamic response of the presented VCIMD is demonstrated in Fig. 7. A smooth transition from the steady state to a transient state is obtained at around  $t = 0.16$  s.

At 0.5 s, when load is varied from 50% of rated torque to 90% of rated torque, there is a change in 3-phase supply current and stator currents of the induction motor. During load variation, it is observed that the IMD responds satisfactorily.

The grid current, grid voltage, and motor stator current of the proposed converter are presented in Figs. 8(a), (c), and (e), respectively. The grid current waveform has a THD of 1.43%, as shown in Fig. 8(b). According to harmonic analysis depicted in Fig. 8(d), the grid voltage waveform has 3.02% THD. The stator current comprises only 2.66% THD, according to the harmonic analysis presented in Fig. 8(f). These values are obtained at 100% of the rated load conditions. These waveforms have improved power quality, and THDs are less than 5%, which is in conformity with IEEE-519.



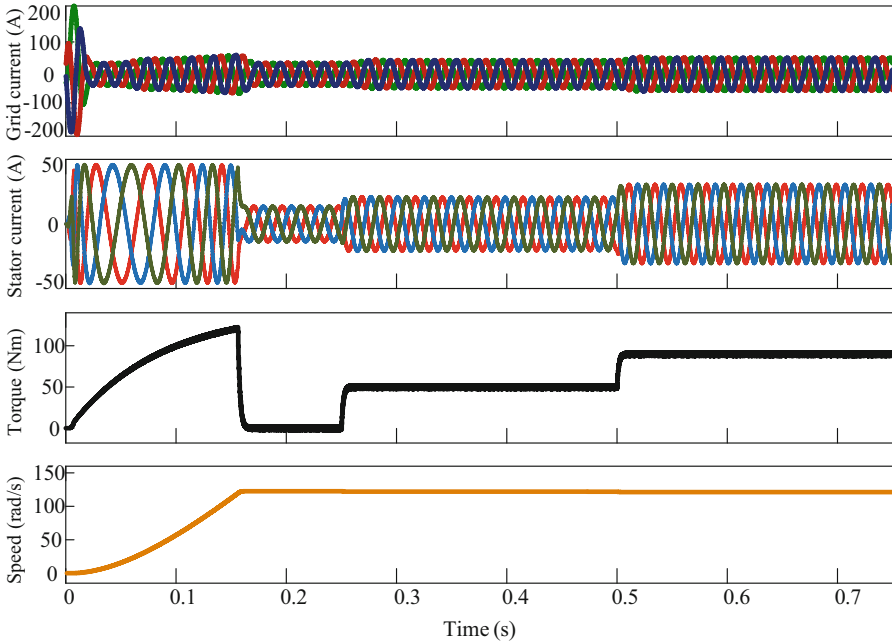


Fig. 7. Dynamic response of the VCIMD.

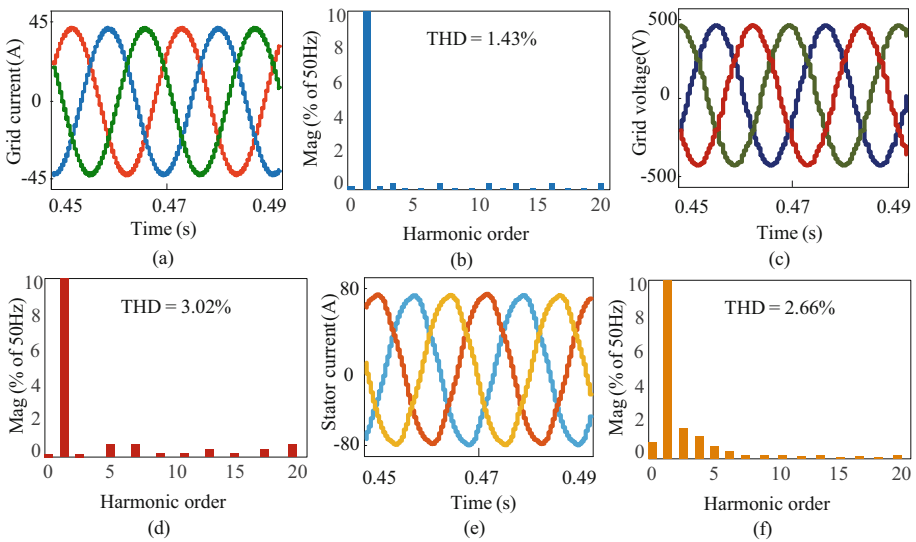


Fig. 8. Analysis of (a) grid current, (b) harmonic spectra of grid current, (c) grid voltage, (d) harmonic spectra of grid voltage, (e) motor stator current, and (f) harmonic spectra of motor stator current.

## 4 Results and Discussion

Table 1 depicts the comparison of several performance metrics between the proposed converter and the conventional 6-pulse converter. The THD of supply voltage ( $V_s$ ) and supply current ( $I_s$ ) of the proposed converter is less than 5%. At light load (LL), the THD of the 6-pulse converter's supply current is 61.8%, and at full load (FL), the THD value is 31.3%. As both the supply voltage and supply current of the 6-pulse converter are more than 5%, they do not meet the IEEE requirements. Moreover, it is evident that the power factor using the proposed configuration is closer to unity than the conventional 6-pulse configuration. Therefore, the improved performance metrics of the presented converter make it suitable for retrofit applications.

**Table 1.** Comparative analysis of power quality parameters.

Configuration	THD of $V_s$ (%)	THD of $I_s$ (%)		DF		DPF		PF	
		LL (20%)	FL (100%)	LL (20%)	FL (100%)	LL (20%)	FL (100%)	LL (20%)	FL (100%)
6-pulse	6.79	61.8	31.3	0.843	0.952	0.949	0.973	0.808	0.932
44-pulse	3.02	1.97	1.43	0.997	0.995	0.987	0.979	0.992	0.993

Table 2 presents how large load variations influence the performance metrics of the IMD. With power factors of 0.9924 and 0.9935, the THD of supply voltage ( $V_s$ ) is 2.43% at light load (LL) and 3.02% at full load (FL). Supply current ( $I_s$ ) has a THD of 1.97% under light load and 1.43% at full load. THDs of both supply voltage and current satisfy the IEEE-519 standard. Both the displacement factor (DPF) and the distortion factor (DF) are within acceptable limits. The power factor (PF) is close to unity in value.

**Table 2.** Power quality parameters under load variation.

Load (%)	THD of $V_s$ (%)	THD of $I_s$ (%)	THD of $I_{st}$ (%)	DF	DPF	PF
20	2.43	1.97	3.94	0.9972	0.9873	0.9924
40	2.76	1.89	3.50	0.9961	0.9854	0.9936
60	2.92	1.73	3.36	0.9965	0.9836	0.9935
80	2.98	1.52	3.05	0.9952	0.9798	0.9932
100	3.02	1.43	2.66	0.9951	0.9792	0.9931

## 5 Conclusion

This work presents a new hexagon-connected transformer with a 44-pulse AC-DC converter fed by VCIMD. The presented converter's design technique has demonstrated the

ability to construct an autotransformer applicable for retrofit applications. The power quality metrics such as THD of the AC main current, THD of the AC main voltage, and power factor have improved employing the proposed converter as compared to the conventional converter. The power factor of the VCIMD is always greater than 0.9924, regardless of the large load variation. As a result, the presented 44-pulse AC-DC converter can efficiently replace the existing 6-pulse converter without requiring major equipment adjustments.

## Appendix

Specification of IMD: Y-connected, 4-pole, 415 V, 50 Hz, 10 hp (7.5 kW), 3- $\phi$  squirrel-cage IM.

DC-link filter:  $L_d = 2$  mH,  $C_d = 2200$   $\mu$ F.

## References

1. Islam, M., Biswas, S.P., Anower, M.S., Islam, M.R., Abu-Siada, A.: An advanced modulation technique for power quality improvement in 12-pulse rectifier-inverter fed induction motor drive. In: Australasian Universities Power Engineering Conference (AUPEC), pp. 1–6. IEEE, Hobart (2020)
2. Biswas, S.P., Anower, M.S., Sheikh, M.R.I., Islam, M.R., Muttaqi, K.M.: Investigation of the impact of different PWM techniques on rectifier-inverter fed induction motor drive. In: Australasian Universities Power Engineering Conference (AUPEC), pp. 1–6. IEEE, Hobart (2020)
3. Singh, B., Garg, V., Bhuvaneswari, G.: Polygon-connected autotransformer-based 24-pulse AC–DC converter for vector-controlled induction-motor drives. *IEEE Trans Ind Electron* **55**(1), 197–208 (2008)
4. Abdollahi, R.: Hexagon-connected transformer-based 20-pulse AC–DC converter for power quality improvement. *J. Electr. Syst.* **8**(2), 119–131 (2012)
5. Singh, B., Gairola, S.: Design and development of a 36-pulse AC-DC converter for vector controlled induction motor drive. In: 7th International Conference on Power Electronics and Drive Systems, pp. 694–701. IEEE, Bangkok (2007)
6. Shila, S., Biswas, S.P., Islam, M.R., Rahman, M.M., Shafiullah, G., Sadaba, O.A.: A new PWM scheme to improve the input power quality of 18-pulse rectifier fed 3-level NPC inverter based induction motor drive. In: 31st Australasian Universities Power Engineering Conference (AUPEC), pp. 1–6. IEEE, Perth (2021)